

# Identifying Few-Molecule Water Clusters with High Precision on Au(111) Surface

Anning Dong,<sup>†,‡,§</sup> Lei Yan,<sup>†,‡,§</sup> Lihuan Sun,<sup>†,‡,§</sup> Shichao Yan,<sup>||</sup> Xinyan Shan,<sup>†,‡</sup> Yang Guo,<sup>†,‡</sup> Sheng Meng,<sup>\*,†,‡,§</sup> and Xinghua Lu<sup>\*,†,‡,§</sup>

<sup>†</sup>Beijing National Laboratory for Condensed-Matter Physics and Institute of Physics, Chinese Academy of Sciences, Beijing, 100190, People's Republic of China

<sup>‡</sup>School of Physical Sciences, University of Chinese Academy of Sciences, Beijing, 100190, People's Republic of China

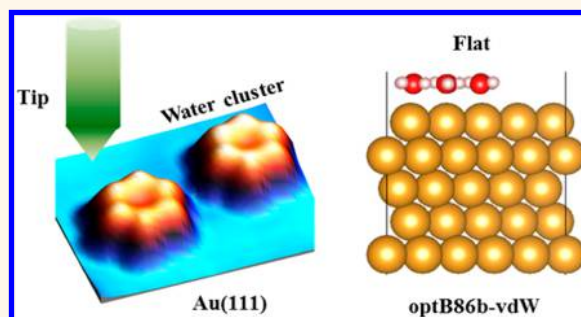
<sup>§</sup>Collaborative Innovation Center of Quantum Matter, Beijing, 100190, People's Republic of China

<sup>||</sup>School of Physical Science and Technology, ShanghaiTech University, Shanghai, 201210, China

## Supporting Information

**ABSTRACT:** Revealing the nature of a hydrogen-bond network in water structures is one of the imperative objectives of science. With the use of a low-temperature scanning tunneling microscope, water clusters on a Au(111) surface were directly imaged with molecular resolution by a functionalized tip. The internal structures of the water clusters as well as the geometry variations with the increase of size were identified. In contrast to a buckled water hexamer predicted by previous theoretical calculations, our results present deterministic evidence for a flat configuration of water hexamers on Au(111), corroborated by density functional theory calculations with properly implemented van der Waals corrections. The consistency between the experimental observations and improved theoretical calculations not only renders the internal structures of adsorbed water clusters unambiguously, but also directly manifests the crucial role of van der Waals interactions in constructing water–solid interfaces.

**KEYWORDS:** scanning tunneling microscope, water clusters, internal structures, density functional theory, van der Waals interactions



The water–solid interface plays an important role in a broad range of phenomena, including corrosion, catalysis, electrochemistry, and life activities.<sup>1–4</sup> A critical step toward fully understanding the water–solid interface is to reveal the microscopic nature of water clusters at the initial stage of water nucleation onto solid surfaces, which includes molecular conformations with atomic details,<sup>5–8</sup> charge hybridization,<sup>9,10</sup> and dynamic behaviors.<sup>11–13</sup> The molecular structure of a water cluster on the surface is mainly determined by the hydrogen-bond interactions between adjacent water molecules and the bonding forces between water molecules and the substrate. Individual water molecules<sup>14</sup> and various clusters including dimers,<sup>15,16</sup> trimers,<sup>17</sup> tetramers,<sup>18,19</sup> hexamers,<sup>6</sup> and other higher order clusters,<sup>9</sup> have been observed and analyzed by scanning tunneling microscope (STM) in conjunction with density functional theory (DFT). On reactive metal surfaces such as Ru and Pd, the water–substrate bonds are normally stronger than the hydrogen bond. The conformation of water molecules and their growth patterns are thus mainly determined by water–metal interactions.<sup>20</sup> On noble metal surfaces, however, the bonding forces between water molecules and substrate become much weaker, and van der Waals (vdW) dispersion forces start to play a significant

role in governing the structure of water clusters and their stabilities. Recent DFT calculations with vdW forces implemented showed that buckled water hexamers are slightly more stable than flat ones on the Cu surface (with an energy difference about 16 meV/H<sub>2</sub>O), while calculations without vdW forces showed a significant preference for buckling (about 120 meV/H<sub>2</sub>O).<sup>21</sup> The role of vdW dispersion forces in determining the adsorption sites and equilibrium structures, as well as the chemical properties of water–solid interfaces, remains a challenge for water science.

This versatility, as a result of the subtle balance between hydrogen-bond interaction and the vdW dispersion forces, has not been fully demonstrated with sufficient experimental data, due to the notorious and long-standing difficulty in imaging water clusters on nonreactive surfaces.<sup>22</sup> When imaged with a normal STM tip, even at cryogenic temperatures, water clusters up to hexamers were normally shown as single protrusions with very little information on their internal structure. To the best of

**Received:** March 26, 2018

**Accepted:** May 29, 2018

**Published:** May 29, 2018

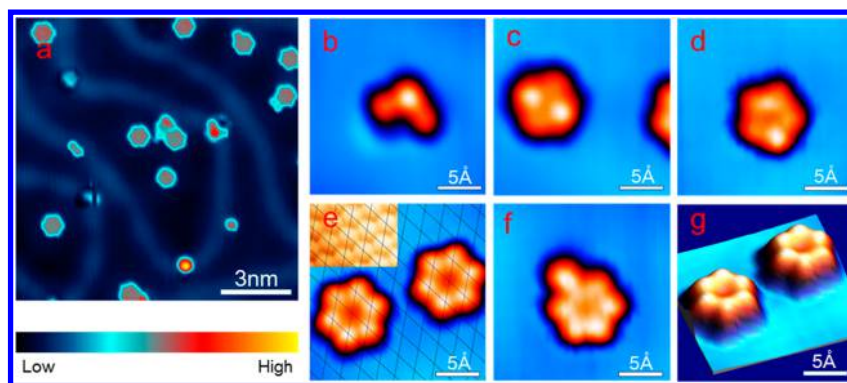


**Figure 1.** Nucleation of water molecules on Au(111). (a) Typical STM image of water clusters on Au(111). Water molecules randomly adsorb on Au(111) surface and form different kinds of nanoclusters. Set point:  $V = -200$  mV,  $I = 50$  pA. Panels b,c,d,e, and f show the fundamental configurations of water trimer, tetramer, pentamer, hexamer, and heptamer, respectively. Set point:  $V = -100$  mV,  $I = 50$  pA. (g) 3D image corresponding to that in panel e. The inset in panel e presents the surface of substrate adjacent to the adsorption sites with atomic resolution, which helps identify the underlying lattice, as demonstrated by the black gridlines. Set point:  $V = -20$  mV,  $I = 50$  pA.

our knowledge, there have been very limited observations that report molecular resolution in water clusters on noble metal surfaces.<sup>6,19,23</sup> There has been a pressing need in visualizing molecular structure in few-molecule water clusters, to justify the balance of hydrogen bonds and vdW dispersion forces in governing water structures on solid surfaces.

Here we report a combined low temperature STM and first-principle calculations to reveal the atomic details of water clusters on Au(111) surface. A series of few-molecule water clusters has been imaged with ultrahigh spatial resolution by water molecule or OH group terminated tip, sufficient to distinguish the adsorption site and height of each molecule in the clusters deterministically. While clusters of trimer, tetramer, and pentamer present buckled configurations, water hexamers are shown in an unambiguous coplanar configuration. Such a coplanar hexamer structure is further evidenced by manipulations with an STM tip. DFT calculations with properly implemented vdW corrections show excellent agreement with the experimental observations. The contribution of vdW interaction in establishing proper water structures on the surface has been clearly demonstrated, providing insights into the microscopic behavior of water nucleation on surfaces and related phenomena.

## RESULTS AND DISCUSSION

When deposited onto the Au(111) surface, water molecules nucleate spontaneously and build a variety of configurations, as shown in Figure 1a. Most of the isolated nanostructures are water clusters comprising a few water molecules. Figure 1 panels b–f present typical STM topographs of a water trimer, tetramer, pentamer, hexamer, and heptamer. No water monomers or dimers were identified, probably due to their relatively high mobility on this surface. From high-resolution topographs of both water clusters and underlying Au(111) substrate, we are able to determine adsorption sites of all water molecules in each cluster; for example, water molecules favor top sites adsorption for hexamers (Figure 1e). It is worth noting that such high-resolution images can be acquired only with a functionalized STM tip. The functionalization was achieved by poking the tip over small water clusters with a sample bias voltage between  $-1$  and  $-3$  V and tip extension by a few angstroms. The most plausible species at the end of the functionalized tip is a water molecule or a hydroxyl group. As long as the STM tip was functionalized, a higher resolution for

STM images was easily achieved compared with normal metallic tips (for details, see Supporting Information, Figure S1).

The most interesting observation is that while water molecules of different heights appear in water trimers, tetramers, and pentamers, the six water molecules in a cyclic hexamer are of exactly the same height. The V-shaped water trimer, with the O–O–O angle of  $110^\circ$ , usually consists of a high-lying ( $1.07$  Å) water molecule in the center and two low-lying ( $0.9$  Å) ones on each side, as shown in Figure 1b. The water tetramer forms a symmetric buckled square ring, as shown in Figure 1c, with two high-lying ( $1.03$  Å) and two low-lying ( $0.89$  Å) water molecules. A flat water tetramer with submolecular resolution has been reported on NaCl(001)/Au(111).<sup>19</sup> The distinction in structure from our observation directly reflects the crucial role of water–solid interactions in determining the adsorption structure of water clusters. The heights of water molecules in a pentamer (Figure 1d) are  $1.03$  and  $0.89$  Å, for high-lying and low-lying molecules, respectively. It is worth noting that we have realized imaging of a single water pentamer with molecular resolution, the geometry of which is highly consistent with the results in quasi-1D ice chains built from a face-sharing arrangement of water pentagons as imaged by STM<sup>24</sup> and AFM.<sup>23</sup> Especially, direct observation of the pentagonal water unit has been presented in AFM images acquired with a CO-functionalized tip.<sup>23</sup> The water molecules in a hexamer (Figure 1e), on the other hand, are of the same height of  $0.9 \pm 0.01$  Å and the corresponding 3D image (Figure 1g) gives a better visual effect. We have carefully examined more than 50 hexamers, and all of them show the same height profile. Derivatives of water hexamers are also observed, such as the water heptamers (Figure 1f). According to the statistics, the most common water species are water hexamers and the number of water clusters with other sizes is relatively fewer, especially for water pentamers which are rarely observed. All the heights mentioned above are the apparent height of water molecules with respect to the underlying surface, and the observed configurations almost show nothing to do with the underlying herringbone reconstructions.

From a microscopic point of view, the hydrogen bond network in a water structure on the solid surface is determined by the competition between water–water and water–solid interactions.<sup>4</sup> Simply, the competition could align to the

number of accepted H bonds in a single water molecule. If a water molecule has already accepted two H-bonds (double acceptor), there is no available molecular orbitals to establish a chemical bond to the surface, because the same molecular orbital ( $1b_1$ ) is involved in the formation of both H-bond and O-metal bond.<sup>7</sup> The double-acceptor water molecules with their plane perpendicular to the surface stay further away from the surface than those water molecules with the O-metal bonds to the surface.<sup>25,26</sup> As discussed above, there are double acceptors in water trimer, tetramer, and pentamer, while all six molecules in a cyclic hexamer are equally bonded to the surface which leads to a coplanar configuration for a water hexamer.

As the basic building block of ice, water hexamers have attracted the most intensive research interest both experimentally and theoretically.<sup>6,26–28</sup> As we are aware, previous results from DFT investigations<sup>6</sup> mostly predict a buckled bilayer structure for a water hexamer on noble metal surfaces (such as Cu(111), Ag(111), *etc.*), with more than 0.5 Å height difference between the alternating molecules. However, such apparent height contrast has never been observed in STM investigations.<sup>29</sup> The topographic images were not adequate, in both quality and quantity, to exclude the buckled model, either. Clearly, STM images with much higher spatial resolution and more evidence are crucial to unravel this ambiguous condition.

Besides the high spatial resolution and statistical fidelity, we provide further evidence first by a direct comparison between a buckled tetramer and a coplanar hexamer side by side in the same topographic image. Figure 2 shows the topograph and the

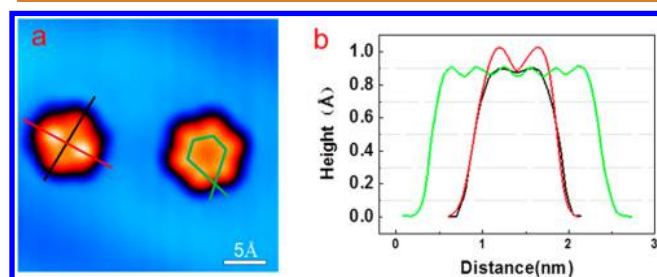


**Figure 2.** Comparison between the buckled tetramer and flat hexamer. (a) STM topograph of buckled tetramer and flat hexamer. (b) Height profiles along line-cuts as indicated in panel a, including the low lying water molecules (black), buckled water molecules (red) in water tetramer, and all water molecules in water hexamer (green). Set point:  $V = -100$  mV,  $I = 50$  pA.

height profiles along the line-cuts in both clusters. It is clear that the water molecules in the hexamer are all of the same

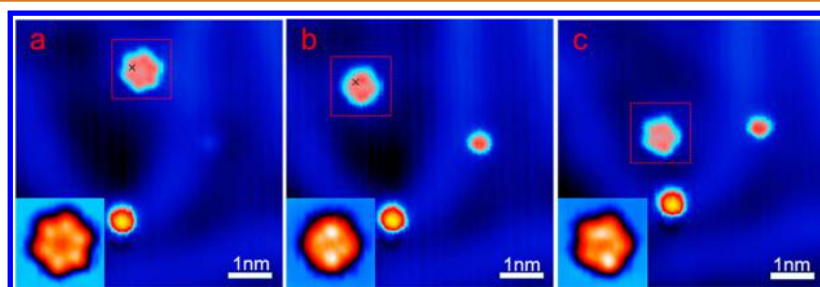


**Figure 3.** Tip induced hydrogen bond network reconfiguration. Consecutive STM images taken after a series of manipulations. (a) A water hexamer, before applying a voltage pulse ( $V = -0.9$  V) at position marked by a cross. (b) STM image after manipulation, including a tetramer and a monomer (diffusing to the defect site). (c) A water pentamer built from the tetramer in panel b, and a water molecule on the STM tip. Scale bar, 1 nm. The insets present zoom-in STM images of areas highlighted by the red dotted lines. Set point:  $V = -100$  mV,  $I = 50$  pA.

height as the lower ones in the tetramer, which indicates that all the molecules in the water hexamer are closely bonded to underlying atoms and present a coplanar configuration. Such a comparison, under exactly the same imaging condition, eliminates possible influences due to the tip changes (even very slight) between different scans, or the tip effects (e.g., local electric field), as well as the time averaging effect.

Second, in order to exclude the possibility of any underlying defects, we successfully manipulated some hexamers to different positions on the surface, where they kept the same coplanar configuration (for details, see Figure S2). Further manipulation shows that a coplanar hexamer can transform into a buckled tetramer or pentamer when the water molecule(s) is extracted from it, as demonstrated in Figure 3. The high-resolution images of each cluster (insets of Figure 3) present a buckled configuration in both tetramer and pentamer, whereas the precursor (the hexamer) shows a coplanar configuration.

Consider this surprising fact that the coplanar hexamer structure as observed in our experiment has never been proposed by previous theoretical investigations, we re-evaluate the validity and sufficiency of previous theoretical models. A series of DFT simulations based on different exchange-correlation functionals have been carried out, including Perdew–Burke–Ernzerhof (PBE),<sup>30</sup> PBE with D2-vdW corrections,<sup>31</sup> and PBE with optB86b-vdW method<sup>32</sup> (for details, see Table S1). Indeed, the widely used DFT-PBE calculations predict a buckled bilayer structure for the water hexamer both in gas phase and on Au(111) surface, agreeing with previous theoretical data.<sup>6</sup> However, as long as the vdW corrections are included, as in both the PBE with D2 and optB86b-vdW methods, a coplanar structure for water hexamer on Au(111) surface is rendered which is in excellent agreement with the experimental observations. This indicates that the vdW interaction between water and metal atoms, which was largely overlooked, plays a central role in determining the final structures of water adsorption on a gold surface.

Figure 4 presents the results of the water tetramer and hexamer on the Au(111) surface calculated with optB86b-vdW functionals. The corresponding simulated STM images (Figure 4b,d) were obtained with the Tersoff–Hamann method<sup>33</sup> using the constant current mode based on calculated electron densities. The water tetramer presents a buckled structure with a displacement of 0.4 Å between oxygen atoms in the  $z$  direction, while the water hexamer, composed of six nearly flat water molecules with all the H-bonds lying nearly parallel to the surface plane, presents a precise coplanar structure (oxygen



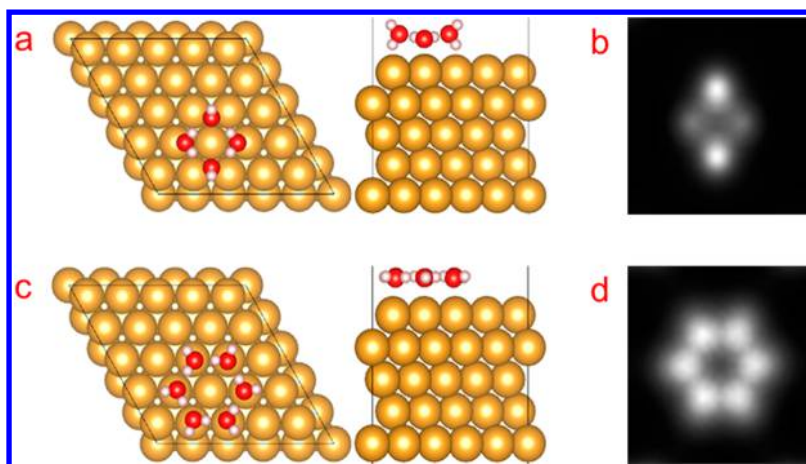


**Figure 4.** DFT simulations of water tetramer and hexamer on Au(111). (a) Top and side view of DFT-calculated structure for tetramer. (b) Simulated STM image of water tetramer, which show an apparent buckled configuration. (c) Top and side view of the calculated hexamer. (d) Simulated STM image of water hexamer, which show an apparent coplanar configuration.

**Table 1.** Adsorption Energies and Structures of Water Hexamer on Au(111) with PBE and optB86b-vdW Functionals<sup>a</sup>

approach	$E_{\text{ads}}$	$E_{\text{a}}(\text{H}_2\text{O})_6/\text{Au}$	$E_{\text{a}}(\text{H}_2\text{O})/\text{Au}$	$\Delta E_{\text{flat}}$	$\Delta E$	$Z(\text{H}_2\text{O})_6/\text{Au}$
PBE	390	28	89	127	-38	0.47, 0.00, 0.48, -0.01, 0.46, -0.02
optB86b-vdW	547	185	281	124	157	0.07, 0.00, 0.06, -0.04, 0.01, -0.05

<sup>a</sup>Compared with the PBE method, the adsorption energy greatly increased after the implementation of vdW corrections, which accounts for the planarization in adsorption structures. The units for energy and height are meV and Å, respectively. Here, averaged adsorption energy is described as  $E_{\text{ads}} = (E_{\text{Au}} + n \times E_{\text{H}_2\text{O}} - E_{(\text{H}_2\text{O})_n/\text{Au}})/n$  and  $E_{\text{a}} = (E_{\text{Au}} + E_{(\text{H}_2\text{O})_n} - E_{(\text{H}_2\text{O})_n/\text{Au}})/n$ , energy difference is defined as  $\Delta E_{\text{flat}} = (E_{(\text{H}_2\text{O})_n} - E_{(\text{H}_2\text{O})_n/\text{flat}})/n$  and  $\Delta E = E_{\text{a}(\text{H}_2\text{O})/\text{Au}} - \Delta E_{\text{flat}}$ , and the relative heights for six water molecules in hexamer are defined as  $Z_{(\text{H}_2\text{O})_6}$ .

height difference  $<0.07$  Å), which is significantly different from previous theoretical calculations.

To explore the reason for this discrepancy, we made a detailed comparison in atomic configurations and adsorption energies calculated with the PBE and optB86b-vdW approaches (for the tetramer case, see Table S2). With the PBE approach, the buckled hexamer is stable with the vertical O–O displacement of  $\sim 0.5$  Å, while the flat hexamers are significantly less stable (by 127 meV/water) than the buckled ones both in gas phase and on metal surface, as seen from the planarization energy per water molecule ( $\Delta E_{\text{flat}}$ ) in Table 1. The adsorption energy of single water molecule ( $E_{\text{a}}[\text{H}_2\text{O}/\text{Au}] = 89$  meV) is lower than the energy of planarization per water molecule ( $\Delta E_{\text{flat}} = 127$  meV). Consequently, the interaction between water molecule and substrate is too weak to conquer the hydrogen-bond interaction for forming a flat structure ( $\Delta E = E_{\text{a}} - \Delta E_{\text{flat}} < 0$ ). In contrast, when vdW correction is taken into consideration (in optB86b-vdW approach), the flat hexamer is more stable than the buckled one, with a planarization energy of 124 meV per water molecule. Adsorption energy per water  $E_{\text{a}}[\text{H}_2\text{O}/\text{Au}]$  is now increased to 281 meV, much larger than  $\Delta E_{\text{flat}}$  which leads to a positive energy difference ( $\Delta E = 157$  meV), in accordance with the average adsorption energy of the water hexamer ( $E_{\text{a}}[(\text{H}_2\text{O})_6/\text{Au}] = 185$  meV). That is, the ability of one water molecule to bind surface is stronger than its ability to accept an additional H-bond. Thus, the coplanar configuration is favored when the vdW interactions are taken into account, which is in excellent agreement with our experimental observations.

The role of vdW dispersion forces in determining wetting behaviors on metals has been investigated in a few previous studies.<sup>34–36</sup> All results presented up to now highlight the crucial role of vdW dispersion forces in enhancing the water–

solid interactions, but usually do not alter the adsorption geometry when compared to the results from PBE functionals.<sup>37–39</sup> Here we find that vdW force is a key factor in constructing correct geometry of water hexamer on gold, with determinant experimental and theoretical evidence.

Our DFT results clearly show that vdW interaction significantly enhances the bonding with substrate and as a result the buckled water hexamers are flattened. The results deduced for Au is also valid for Ag (Figure S3a,b). For Cu, although the water hexamer still has a slight preference for buckled configuration (Figure S3c,d), the energy difference reduced to 22 meV/H<sub>2</sub>O (Table S3), which is consistent with the results in ref 21. Our calculations suggest that the vdW dispersion forces could alter the adsorption structure by enhancing water-metal bonding, which leads to a preference for flat water clusters. As the basic building block, the flattening of the water hexamer may have far-reaching impact on the epitaxial growth of the first water layer such as the size, geometry, and stability, which are of great importance but remain unclear. Thus, further studies on the formation of first water layer and multilayers are urgently needed.

## CONCLUSIONS

In summary, we have realized molecular-resolved STM imaging in a series of water clusters ranging from trimers to heptamers. Our results provide deterministic evidence for the coplanar configuration of water hexamers, while other clusters present a buckled geometry implying the existence of double acceptors. The comparison to DFT calculations with different exchange-correlation functionals manifests the crucial role of vdW dispersion forces in constructing correct adsorption structures at water–solid interfaces. It is bound to facilitate our understanding on the competition and subtle balance between

water–water and water–solid interactions, hence hints for the microscopic mechanisms for ice nucleation, epitaxy growth of ice films, and chemical properties of water–solid interfaces.

## METHODS

The experiment was carried out in a home-built low-temperature STM with base pressure lower than  $3.0 \times 10^{-11}$  Torr. The Au(111) substrate was prepared by repeated cycles of sputtering and annealing until a clean Au(111)- $22 \times \sqrt{3}$  reconstructed surface was obtained. Water molecules were deposited onto the surface of the Au(111) crystal hold at the cold STM stage around 19 K; the detailed method has been introduced previously.<sup>9</sup> The tungsten tip was prepared by electrochemical etching, resulting in a typical radius of curvature about 20 nm. The functionalization was achieved by poking the tip over small water clusters with a voltage pulse (typically  $-2$  V with 200 ms duration) and tip extension by a few angstroms. Measurements were carried out at 19 K by using a scan bias no more than 200 mV for stable imaging.

DFT calculations were performed in the VASP code,<sup>40</sup> employing semilocal exchange–correlation functionals and PAW<sup>41</sup> pseudopotentials. van der Waals corrections for dispersion forces were considered within the vdW-DF scheme using the optB86b-vdW method.<sup>32</sup> The substrate consists of five-layers of Au(111) atomic slabs with a bulk lattice constant of 3.99 Å estimated from experimental values. A ( $5 \times 5$ ) supercell was used to accommodate the water clusters. All the structures were fully relaxed with the bottom four layers of Au atoms fixed. The vacuum region of more than 10 Å in the  $z$  direction was applied, which is sufficiently large to eliminate the artificial periodic interaction, and the Brillouin zone was sampled by  $2 \times 2 \times 1$  Monkhorst–Pack  $k$ -mesh. The cutoff energy of plane-wave basis was taken at 400 eV, and the geometries of the water/Au(111) systems were optimized until the force on each atom was less than 0.03 eV/Å. The simulated STM images were obtained with the Tersoff–Hamann method<sup>33</sup> using the constant current mode based on calculated electron densities.

## ASSOCIATED CONTENT

### Supporting Information

The Supporting Information is available free of charge on the ACS Publications website at DOI: 10.1021/acsnano.8b02264.

Process of tip functionalization; manipulations of water hexamer on Au; adsorption energies and structures of water hexamer on Au with different functionals; water tetramer with PBE and optB86b-vdW methods; detailed comparison of adsorption energy between the flat and buckled water hexamers on Cu and Ag using different methods (PDF)

## AUTHOR INFORMATION

### Corresponding Authors

\*E-mail: smeng@iphy.ac.cn. Phone: +861082649396.

\*E-mail: xhlu@iphy.ac.cn. Phone: +861082648043.

### ORCID

Anning Dong: 0000-0002-3145-7228

Lei Yan: 0000-0002-2698-4613

Lihuan Sun: 0000-0002-4259-3313

Sheng Meng: 0000-0002-1553-1432

Xinghua Lu: 0000-0003-4228-0592

### Notes

The authors declare no competing financial interest.

## ACKNOWLEDGMENTS

We acknowledge the financial support from National Natural Science Foundation of China under Grant Nos. 11774395,

11727902, 11474328, 11774396 and 61376100, Beijing Natural Science Foundation under Grant No. 4181003, Ministry of Science and Technology of China under Grant No. 2012CB933002 and 2016YFA0300902, Strategic Priority Research Program (B) of the Chinese Academy of Sciences under Grant Nos. XDB07030100 and XDPB06, Chinese Academy of Sciences under Grant No. 07C3021B51. We thank D. Hao and J. Li for constructive discussions.

## REFERENCES

- (1) Thiel, P. A.; Madey, T. E. The Interaction of Water with Solid Surfaces: Fundamental Aspects. *Surf. Sci. Rep.* **1987**, *7*, 211–385.
- (2) Henderson, M. A. The Interaction of Water with Solid Surfaces: Fundamental Aspects Revisited. *Surf. Sci. Rep.* **2002**, *46*, 1–308.
- (3) Hodgson, A.; Haq, S. Water Adsorption and the Wetting of Metal Surfaces. *Surf. Sci. Rep.* **2009**, *64*, 381–451.
- (4) Meng, S.; Wang, E. G.; Gao, S. Water Adsorption on Metal Surfaces: A General Picture from Density Functional Theory Studies. *Phys. Rev. B: Condens. Matter Mater. Phys.* **2004**, *69*. DOI: 10.1103/PhysRevB.69.195404
- (5) Verdaguier, A.; Sacha, G. M.; Bluhm, H.; Salmeron, M. Molecular Structure of Water at Interfaces: Wetting at the Nanometer Scale. *Chem. Rev.* **2006**, *106*, 1478–1510.
- (6) Michaelides, A.; Morgenstern, K. Ice Nanoclusters at Hydrophobic Metal Surfaces. *Nat. Mater.* **2007**, *6*, 597–601.
- (7) Carrasco, J.; Hodgson, A.; Michaelides, A. A Molecular Perspective of Water at Metal Interfaces. *Nat. Mater.* **2012**, *11*, 667–674.
- (8) Maier, S.; Lechner, B. A. J.; Somorjai, G. A.; Salmeron, M. Growth and Structure of the First Layers of Ice on Ru(0001) and Pt(111). *J. Am. Chem. Soc.* **2016**, *138*, 3145–3151.
- (9) Guo, Y.; Ding, Z.; Sun, L.; Li, J.; Meng, S.; Lu, X. Inducing Transient Charge State of a Single Water Cluster on Cu(111) Surface. *ACS Nano* **2016**, *10*, 4489–95.
- (10) Hammer, N. I.; Shin, J.-W.; Headrick, J. M.; Diken, E. G.; Roscioli, J. R.; Weddle, G. H.; Johnson, M. A. How Do Small Water Clusters Bind an Excess Electron? *Science* **2004**, *306*, 675–679.
- (11) Gawronski, H.; Carrasco, J.; Michaelides, A.; Morgenstern, K. Manipulation and Control of Hydrogen Bond Dynamics in Adsorbed Ice Nanoclusters. *Phys. Rev. Lett.* **2008**, *101*, 136102.
- (12) Kumagai, T.; Shiotari, A.; Okuyama, H.; Hatta, S.; Aruga, T.; Hamada, I.; Frederiksen, T.; Ueba, H. H-Atom Relay Reactions in Real Space. *Nat. Mater.* **2012**, *11*, 167–172.
- (13) Mehlhorn, M.; Carrasco, J.; Michaelides, A.; Morgenstern, K. Local Investigation of Femtosecond Laser Induced Dynamics of Water Nanoclusters on Cu(111). *Phys. Rev. Lett.* **2009**, *103*, 026101.
- (14) Mitsui, T.; Rose, M.; Fomin, E.; Ogletree, D. F.; Salmeron, M. Water Diffusion and Clustering on Pd(111). *Science* **2002**, *297*, 1850–1852.
- (15) Motobayashi, K.; Matsumoto, C.; Kim, Y.; Kawai, M. Vibrational Study of Water Dimers on Pt(111) Using a Scanning Tunneling Microscope. *Surf. Sci.* **2008**, *602*, 3136–3139.
- (16) Motobayashi, K.; Árnadóttir, L.; Matsumoto, C.; Stuve, E. M.; Jónsson, H.; Kim, Y.; Kawai, M. Adsorption of Water Dimer on Platinum(111): Identification of the  $-OH \cdots Pt$  Hydrogen Bond. *ACS Nano* **2014**, *8*, 11583–11590.
- (17) Kumagai, T.; Okuyama, H.; Hatta, S.; Aruga, T.; Hamada, I. Water Clusters on Cu(110): Chain versus Cyclic Structures. *J. Chem. Phys.* **2011**, *134*, 024703.
- (18) Okuyama, H.; Hamada, I. Hydrogen-Bond Imaging and Engineering with a Scanning Tunneling Microscope. *J. Phys. D: Appl. Phys.* **2011**, *44*, 464004.
- (19) Guo, J.; Meng, X.; Chen, J.; Peng, J.; Sheng, J.; Li, X.-Z.; Xu, L.; Shi, J.-R.; Wang, E.; Jiang, Y. Real-Space Imaging of Interfacial Water with Submolecular Resolution. *Nat. Mater.* **2014**, *13*, 184–189.
- (20) Tatarokhanov, M.; Ogletree, D. F.; Rose, F.; Mitsui, T.; Fomin, E.; Maier, S.; Rose, M.; Cerdá, J. I.; Salmeron, M. Metal- and

Hydrogen-Bonding Competition During Water Adsorption on Pd (111) and Ru (0001). *J. Am. Chem. Soc.* **2009**, *131*, 18425–18434.

(21) Liriano, M. L.; Gattinoni, C.; Lewis, E. A.; Murphy, C. J.; Sykes, E. C. H.; Michaelides, A. Water–Ice Analogues of Polycyclic Aromatic Hydrocarbons: Water Nanoclusters on Cu (111). *J. Am. Chem. Soc.* **2017**, *139*, 6403–6410.

(22) Guo, J.; Bian, K.; Lin, Z.; Jiang, Y. Perspective: Structure and Dynamics of Water at Surfaces Probed by Scanning Tunneling Microscopy and Spectroscopy. *J. Chem. Phys.* **2016**, *145*, 160901.

(23) Shiotari, A.; Sugimoto, Y. Ultrahigh-Resolution Imaging of Water Networks by Atomic Force Microscopy. *Nat. Commun.* **2017**, *8*, 14313.

(24) Carrasco, J.; Michaelides, A.; Forster, M.; Haq, S.; Raval, R.; Hodgson, A. A One-Dimensional Ice Structure Built from Pentagons. *Nat. Mater.* **2009**, *8*, 427–431.

(25) Cerda, J.; Michaelides, A.; Bocquet, M. L.; Feibelman, P. J.; Mitsui, T.; Rose, M.; Fomin, E.; Salmeron, M. Novel Water Overlay Growth on Pd(111) Characterized with Scanning Tunneling Microscopy and Density Functional Theory. *Phys. Rev. Lett.* **2004**, *93*, 116101.

(26) Michaelides, A. Simulating Ice Nucleation, One Molecule at a Time, with the ‘DFT Microscope’. *Faraday Discuss.* **2007**, *136*, 287.

(27) Morgenstern, K.; Rieder, K.-H. Formation of the Cyclic Ice Hexamer *via* Excitation of Vibrational Molecular Modes by the Scanning Tunneling Microscope. *J. Chem. Phys.* **2002**, *116*, 5746.

(28) Morgenstern, K.; Nieminen, J. Intermolecular Bond Length of Ice on Ag(111). *Phys. Rev. Lett.* **2002**, *88*, 066102.

(29) Bjorneholm, O.; Hansen, M. H.; Hodgson, A.; Liu, L. M.; Limmer, D. T.; Michaelides, A.; Pedevilla, P.; Rossmeisl, J.; Shen, H.; Tocci, G.; Tyrode, E.; Walz, M. M.; Werner, J.; Bluhm, H. Water at Interfaces. *Chem. Rev.* **2016**, *116*, 7698–726.

(30) Perdew, J. P.; Burke, K.; Ernzerhof, M. Generalized Gradient Approximation Made Simple. *Phys. Rev. Lett.* **1996**, *77*, 3865.

(31) Lee, K.; Murray, É. D.; Kong, L.; Lundqvist, B. I.; Langreth, D. C. Higher-Accuracy van der Waals Density Functional. *Phys. Rev. B: Condens. Matter Mater. Phys.* **2010**, *82*, 081101.

(32) Klimeš, J.; Bowler, D. R.; Michaelides, A. Van der Waals Density Functionals Applied to Solids. *Phys. Rev. B: Condens. Matter Mater. Phys.* **2011**, *83*. DOI: [10.1103/PhysRevB.83.195131](https://doi.org/10.1103/PhysRevB.83.195131)

(33) Tersoff, J.; Hamann, D. R. Theory of the Scanning Tunneling Microscope. *Phys. Rev. B: Condens. Matter Mater. Phys.* **1985**, *31*, 805–813.

(34) Hamada, I.; Lee, K.; Morikawa, Y. Interaction of Water with a Metal Surface: Importance of van der Waals Forces. *Phys. Rev. B: Condens. Matter Mater. Phys.* **2010**, *81*. DOI: [10.1103/PhysRevB.81.115452](https://doi.org/10.1103/PhysRevB.81.115452)

(35) Nadler, R.; Sanz, J. F. Effect of Dispersion Correction on the Au (1 1 1)-H<sub>2</sub>O Interface: A First-Principles Study. *J. Chem. Phys.* **2012**, *137*, 114709.

(36) Hamada, I.; Meng, S. Water Wetting on Representative Metal Surfaces: Improved Description from van der Waals Density Functionals. *Chem. Phys. Lett.* **2012**, *521*, 161–166.

(37) Carrasco, J.; Santra, B.; Klimes, J.; Michaelides, A. To Wet or Not to Wet? Dispersion Forces Tip the Balance for Water Ice on Metals. *Phys. Rev. Lett.* **2011**, *106*, 026101.

(38) Carrasco, J.; Klimeš, J.; Michaelides, A. The Role of van der Waals Forces in Water Adsorption on Metals. *J. Chem. Phys.* **2013**, *138*, 024708.

(39) Peköz, R.; Donadio, D. Dissociative Adsorption of Water at (211) Stepped Metallic Surfaces by First-Principles Simulations. *J. Phys. Chem. C* **2017**, *121*, 16783–16791.

(40) Kresse, G.; Furthmüller, J. Efficient Iterative Schemes for *ab initio* Total-Energy Calculations Using a Plane-Wave Basis Set. *Phys. Rev. B: Condens. Matter Mater. Phys.* **1996**, *54*, 11169–11186.

(41) Blöchl, P. E. Projector Augmented-Wave Method. *Phys. Rev. B: Condens. Matter Mater. Phys.* **1994**, *50*, 17953.